

THE PENNSYLVANIA STATE UNIVERSITY
SCHREYER HONORS COLLEGE

DEPARTMENT OF GEOSCIENCES

THE ROLE OF SEDIMENT GRAIN SIZE AND BEDROCK ABUNDANCE IN SETTING
THE MORPHOLOGY OF HEADWATER CHANNELS IN MCKITTRICK CANYON IN THE
GUADALUPE MOUNTAINS, NM/TX USA

EMILY LOUCKS
SPRING 2020

A thesis
submitted in partial fulfillment
of the requirements
for a baccalaureate degree
in Geosciences
with honors in Geoscience

Reviewed and approved* by the following:

Roman DiBiase
Assistant Professor of Geosciences
Thesis Supervisor

Peter Heaney
Professor of Geosciences
Honors Adviser

* Electronic approvals are on file.

ABSTRACT

Headwater channels represent a significant portion of watershed relief within steep landscapes, and thus play a key role in the long-term topographic development of mountain ranges. Headwater channels are thought to be sculpted by debris flows, which are poorly understood compared to hillslope or fluvial processes, and no framework exists to relate the morphology of headwater channels to climate, tectonics, or rock strength. Here I analyze headwater channels in the tectonically inactive Guadalupe Mountains of New Mexico and Texas, where systematic variations in bedrock lithology present an excellent opportunity to investigate how rock strength influences the morphology of headwater channels. The lithologic gradient corresponds to the progressive exposure of a massively bedded progradational reef unit moving stratigraphically up section from west to east.

The lithologic transition to less fractured, massive cliff units results in an increase in grain size supplied to the channels and increased exposure of bedrock in the channels and in the catchment. I used 1 m lidar topography to extract channel longitudinal stream profiles and measure channel gradient. I analyzed the connection between headwater channel gradient and bedrock exposure on hillslopes and in channels mapped from high resolution (10 cm) imagery and sediment grain size measured in the field. I find that headwater channel gradient is sensitive to both the increasing trend of bedrock exposure and grain size along the WNW-ESE lithologic gradient, but the slope of channels appears more sensitive to the fraction of bedrock rather than the grain size. This study suggests that headwater channels in threshold landscapes become increasingly sensitive to spatial variability in the underlying bedrock of the hillslopes, set by stratal architecture of the lithologic units in McKittrick Canyon.

TABLE OF CONTENTS

LIST OF FIGURES	iii
LIST OF TABLES	iv
ACKNOWLEDGEMENTS	v
Chapter 1: Introduction	1
Motivation	1
Study Area	4
Chapter 2: Methods	7
2.1 Bedrock Mapping	7
2.2 Hillslope Morphology	8
2.3 Channel Morphology/Extraction	8
2.4 Grain Size Analysis	9
Chapter 3: Results	11
3.1 Bedrock mapping	11
3.2 Hillslope morphology	11
3.3 Channel morphology	12
3.4 Grain size of tributaries	12
Chapter 4: Discussion	13
4.1 Sensitivity of headwater channel slope to grain size and bedrock abundance	13
4.2 Rock strength control on bedrock exposure	14
4.3 Lithologic control on bedrock exposure and fracture spacing in McKittrick Canyon	15
Chapter 5: Conclusion	17
BIBLIOGRAPHY	18

LIST OF FIGURES

- Figure 1: Grain size analysis conducted for 7 of the catchments (excluding 4) with the median grain size (D_{50}) calculated for for each survey. Detailed bedrock mapping of the hillslopes and channels of the 8 catchments outlined in red polygons at a ~50 cm scale resolution. The star symbols represent location of photographs in Figure 3A and Figure 3B.23
- Figure 2: Panorama of McKittrick Canyon (modified from Tinker et al., 1998) with the extent outlined in the overview map (Figure 1) by the cross section of A-A'. Top panel shows the transition from small, even beds in the WNW to more massive reef units in the ESE. Bottom panel outlines the prograding Capitan Reef (purple) that shifts higher into the catchments with distance to the ESE.24
- Figure 3: Location of pictures located at the star symbols on Figure 1. The NW end of McKittrick Canyon has laterally continuous, 2-5 meter tall bedrock cliffs (A) that transition into massive reef units up to 100 meters tall in the SE end of the canyon (B).25
- Figure 4: Bedrock mapping consisted of using the aerial imagery (far left panel) to identify areas of exposed bedrock and outline in a polygon to calculate the slope of the partitioned catchment using the slope map (far right panel)26
- Figure 6: Partitioning of the channels based on the intersection of the channel segments with bedrock map. To classify as a bedrock channel, a majority of the channel segment must overly mapped bedrock.28
- Figure 7:** Structure-from-Motion derived orthomosaic image of sediment patch with a 0.5 m grid spacing overlain. Purple lines indicate measurements of apparent intermediate axis diameter.29
- Figure 8: Fraction of bedrock vs distance downstream from catchment 1 along WNW-ESE lithologic gradient. The fraction of the catchment underlain by the Capitan reef is included on the plot to show how the abundance of bedrock changes with the presence of the reef. 30
- Figure 9: Median grain size, D_{50} , versus Distance Downstream of Catchment 1 along WNW-ESE gradient in lithology. No grain size data available for Catchment 4.31
- Figure 10: (A) Mean Channel Slope versus Median grain size, D_{50} , for the partitioned channels to see how slope changes compared to the grain size in each catchment. (B) Mean Channel Slope versus Fraction of bedrock for the partitioned channels to see how the slope changes for with bedrock exposure.32
- Figure 11: Kernel density plots of channel slope angle separated by whether the catchments contain the Capitan reef (Top panel) or do not contain the reef (bottom panel). The dashed line represents the mean angle of the partitioned channel slopes. Area under the curve represents the abundance of slopes classified as either bedrock or sediment-mantled.33
- Figure 12: Mean catchment slope versus mean channel slope for McKittrick Canyon data compared against data in Southern California (DiBiase et al., 2012). Dashed line represents a 1:1 relationship. The channel slope for DiBiase et al., 2012 is calculated by using a linear fit to each colluvial channel in the catchments, and averaging all such channels for each

catchment, weighted by mean channel length. McKittrick Canyon data averages over all channel segments in a given catchment, weighted by mean channel length.....34

Figure 13: Mean Catchment slope vs percent bedrock exposure for McKittrick Canyon data (Table 1) compared to data from Southern California in the Eastern San Gabriel Mountains (ESGM) and Northern San Jacinto Mountains (NSJM) (Neely et al., 2019).....35

LIST OF TABLES

Table 1: Median grain size, partitioned hillslope morphology, and partitioned channel morphology.22

ACKNOWLEDGEMENTS

I am incredibly grateful for my thesis advisor, Roman DiBiase, for providing me with amazing opportunities the 2.5 years I have been involved in his lab. Roman introduced me to the field of geomorphology and has challenged me mentally (and even physically) in his classes and research projects to grow as a geologist. He has been an invaluable mentor, offering wisdom and advice throughout my college career that has guided me to graduation with the confidence to pursue a Master's degree once I leave Penn State.

I have so many thanks to give to the graduate students in the DiBiase Geomorphology lab. Al Neely, Julia Carre, Joanmarie Del Vecchio, and Perri Silverhart have been incredible mentors since my start in the lab. Every person in the lab has been patient and willing to answer all my questions, even with the most basic software tasks that I couldn't google my way through.

I am especially thankful for Al Neely, whom I have closely worked with for the majority of my time in the lab. Al has always amazed me with his immense knowledge and insightful comments helping me write this thesis. He is one of the most patient people I have had the opportunity to work with, not only in the classroom but also in the field. He has gone above and beyond helping me complete this project, and I am incredibly grateful for all of his help.

I want to thank the Schreyer Honors College for the funding that made it possible to complete the field work for this project, the National Center for Airborne Laser Mapping (NCALM) for flying the lidar used in this project, and the partial support from the National Science Foundation grant EAR-1608014 to R. DiBiase.

Chapter 1: Introduction

Motivation

Landscape morphology emerges from the interaction of tectonic processes that generally increase topographic relief through rock uplift and climate-driven erosion and weathering processes that transport sediment and act to lower topographic relief (Hack, 1960; Ahnert, 1970). In unglaciated landscapes, incision of channel networks generates topographic relief that sets the base-level of hillslopes and channels serve as the main conduits that remove sediment from mountain landscapes. Channel incision is particularly sensitive to channel morphology, hydrology, and the strength of the underlying bedrock (Howard, 1994; Sklar and Dietrich, 2001), and as a result, channel incision into bedrock plays an important part in setting the relief of the landscape and coupling landscape morphology to changes in climate and tectonics (Howard, 1994; Kirby and Whipple, 2012). The presence of headwater channels in steep landscapes is typically overlooked in river incision models, but this process change to debris flow dominated channels may have important implications for landscape evolution (Stock and Dietrich, 2003).

Headwater channels reflect a mixture of hillslope and fluvial processes (Benda, 2005), which means that these channels may not respond to tectonic or climactic perturbations in the same way we would predict for hillslope or fluvial models. Landscape evolution models typically use river incision models that exploit the characteristic concave form of fluvial longitudinal profiles to infer tectonic information based on the relationship between drainage area and slope, known as the stream power law (Howard, 1994; Whipple and Tucker 1999), but

the application of these models is limited to drainage areas greater than $\sim 5 \text{ km}^2$, where fluvial processes dominated (Penserini et al., 2017). In steep, mountainous landscapes, a change to debris flow mechanics may be linked to channel morphology at the field-scale, where headwater channels have a distinct topographic signature from fluvial channels (Stock and Dietrich, 2003). Debris-flow-dominated channels comprise a significant amount of the channel network in steep, mountainous landscapes (Benda et al., 2005) and erosion by debris flows has the potential to limit topographic relief more so than fluvial processes (Stock and Dietrich, 2006), which means that this process change from fluvial to debris flow dominated channels may play an important role in setting the relief of landscapes.

A distinct break in channel longitudinal profiles often exists at the transition point where fluvial channels transitions to debris-flow dominated channels, seen in a more linear longitudinal profile for headwater channels (Lague and Davy, 2003; Stock and Dietrich, 2003; DiBiase et al., 2012), compared to fluvial channels which have a characteristic concave-upwards longitudinal profile, where the slope scales with drainage area in a power-law relationship. Laboratory flume experiments and numerical simulations have also shown that bedrock erosion and sediment transport in debris flows is distinct from that of fluvial processes (Hsu et al., 2008; Yohannes et al., 2012; Prancevic et al., 2014).

Sediment delivery by debris flow occurs from a stochastic process due to the failure of stored sediment that is evacuated following storms (Benda and Dunne 1997) and entrains loose material as it moves down the channel and erodes the channel bed by particle impacts rather than abrasion by sliding, with the magnitude of erosion dependent on the size of the entrained grains rather than the abundance of impacts (Yohannes et al., 2012). The stochastic nature of debris flows makes it challenging to connect observations from controlled flume experiments to natural

landscapes. Additionally, natural landscapes contain significant variability in rock type, sediment grain size, and climate forcing that controls sediment transport. A framework connecting the morphology of debris-flow dominated channels to parameters like climate, tectonics, or rock strength is lacking. Prior flume results or empirical comparisons of headwater channel morphology provide few constraints on how changes in rock type affect the morphology of steep, headwater channels.

Landscape-scale rock strength of the hillslopes plays a fundamental role in landscape evolution by resisting erosive forces (Clarke and Burbank, 2011) and limiting the relief of mountain ranges (Schmidt and Montgomery, 1995). The ability of streams to erode is sensitive to the strength of the underlying bedrock, from a mechanistic standpoint where harder rock is more difficult to abrade (Sklar and Dietrich, 2004), and the strength of bedrock on the hillslopes influences the onset of bedrock exposure and grain size of sediment entering the channel. Rock strength influences the fracture spacing on bedrock cliffs, which influences the size of sediment input into the channels (Sklar et al 2017; DiBiase et al 2018), and can be linked to the slope of fluvial channels (Attal et al., 2015; Shobe et al., 2016). In contrast, studies have found that the slope of sediment-mantled hillslopes are insensitive to changes in the grain size (DiBiase et al 2018). As a result, there is an important dynamic between rock properties on the hillslopes and ensuing grain size that enters the channels plays an important part in controlling the morphology of bedrock rivers (Sklar and Dietrich., 2004). This important dynamic for the slope of river channels has not been studied for the morphology of debris-flow dominated channels, which directly receives sediment from proximal hillslopes.

This study aims to address this knowledge gap by determining how a gradient in rock properties (set by the changing lithology) influences the morphology of headwater channels in

McKittrick Canyon in the Guadalupe Mountains of New Mexico and Texas, USA. I exploit a gradient in apparent rock strength in McKittrick Canyon that is expressed as smaller, more fractured cliffs in the WNW that transitions to massive, less fractured reef units in the ESE. The ESE transition to a larger fraction of hillslopes underlain by a massive carbonate reef unit that forms large cliffs additionally contributes larger grains to the channel network. Along this gradient, I compare how headwater channel morphology responds to differences in underlying bedrock lithology and the grain size of sediment delivered from hillslopes. Using high-resolution lidar topography, field surveys of surface sediment grain size, and 10 cm aerial imagery for McKittrick Canyon, I measure the slope of headwater channels and compare channel slopes to the abundance of bedrock waterfalls exposed in the channel network, the slope of waterfalls exposed in the channel network, and the grain size of sediment mantling headwater channels. Through this approach, I isolate the relative influence of sediment grain size and bedrock exposure on headwater channel gradient.

Study Area

The Guadalupe Mountains of New Mexico and Texas consist of exhumed Permian strata that records deposition on the northwest shelf of the Delaware Basin (Smith and Kerans, 2018). McKittrick Canyon (Figure 1), the focus of this study, represents a complete shelf to basin outcrop of carbonate-siliciclastic sequences that is exposed within a ~5 km transect from WNW-ESE (Figure 2). During the Upper Permian in the Guadalupian time (~255-251 Ma), the basin was characterized by the growth of extensive carbonate reefs that separated the deep ocean basin from a shallow backreef shelf lagoon. Over time the reef grew steadily upward and basinward,

which is seen today in the exposed progradational reef in McKittrick Canyon. The canyon is composed of a backreef in the WNW that consists of interbedded carbonates and siliciclastic, transitioning into a massively bedded Permian reef complex in the ESE that is called the Capitan Formation (Figure 2). The reef complex was subsequently exhumed and has been tectonically stable since the Miocene (Hill, 2000).

The Guadalupe Mountains experience a semi-arid climate with mild winters and hot summers. During the hot season from May to September the mean temperature around 28 °C with the coldest season during November to February with temperatures around 1-11 °C (U.S National Park Service). The Guadalupe Mountains have a mean annual precipitation around 450 mm/year with most of the rain accumulating during the warm summer months. While the Guadalupe Mountains can have variable climate at elevation, the study site in McKittrick Canyon is within a small area (~50 km²) and a narrow elevation range (1500-2300 m) so I assume uniform climate across the study area.

McKittrick canyon is an ideal place to study the influence of rock properties on topography because there is a WNW-ESE gradient in lithology that creates a gradient in rock strength from the transition from small interbedded siliciclastic and dolomitic units to massive carbonate reef units. The massive carbonate units that compose the Capitan Formation are much less fractured and appear to have a stronger intact rock strength than the backreef units in the NW (Figure 3). The change in lithology spans only a few kilometers, which allows for isolation of how channel morphology responds to differences in rock strength. McKittrick Canyon has no knickpoints in its main channel, which in combination with its tectonically inactive setting suggests that baselevel fall and hillslope erosion are steady (Kirby and Whipple, 2012). As a result, I assume that McKittrick Canyon is not responding to tectonic perturbations, has uniform

erosion, and a consistent climate, which isolates bedrock lithology controls on erosional processes along the canyon.

Chapter 2: Methods

2.1 Bedrock Mapping

I chose 8 catchments for mapping based on their location along the lithologic gradient (Figure 1) in the canyon from interbedded, laterally continuous beds in the WNW to massive reef units in the ESE with the catchments varying in the amount of bedrock exposure and steepness. I distinguished between bare-bedrock and soil-mantled hillslopes using 10 cm aerial imagery and a lidar-derived 1 m digital elevation model (DEM) to map areas with outcropping, in place bedrock (Figure 4) (Neely, 2019; Neely et al., 2019). The mapping was performed at a ~50 cm resolution to capture the finest scale resolvable from the imagery data. Everything else outside the bedrock mapping, including vegetation and loose sediment, was classified as “soil/sediment cover”. This mapping thus partitioned the landscape into bedrock hillslopes and soil-mantled hillslopes, which then allows for quantifying how the abundance of bedrock hillslopes changes along the 8 catchments spanning the lithologic gradient (Figure 1).

We determined the fraction of bedrock in the catchments, $F_{\text{catchment}}$, by taking the total area of the bedrock hillslopes, A_{Br} , and dividing by the total drainage area, A_{Dr} :

$$F_{\text{Catchment}} = \frac{A_{Br}}{A_{Dr}}. \quad (1)$$

The fraction of catchment underlain by the reef, F_{reef} , was determined by using the georeferenced USGS Geologic Map of McKittrick Canyon (https://ngmdb.usgs.gov/Prodesc/proddesc_4205.htm) to trace the outline of the Capitan reef onto the lidar DEM (Figure 5). I calculated the area of the reef within the catchment, A_{reef} , and divided this number by the total drainage area of the catchment, A_{Dr} .

$$F_{reef} = \frac{A_{reef}}{A_{Dr}}. \quad (3)$$

2.2 Hillslope Morphology

The hillslope morphology for each catchment was calculated by creating a slope map of the 1 m DEM, where slope is measured as the maximum slope angle from a cell to one of its eight neighbors (Figure 4). The slope calculations were performed for the entire catchment and for bare-bedrock and soil mantled hillslopes independently by partitioning the landscape into each category based on the bedrock mapping (Neely et al., 2019). We extracted the slope map from the bedrock map to obtain the mean hillslope angle of bedrock hillslopes and did the same procedure for the soil mantled hillslopes.

2.3 Channel Morphology/Extraction

The stream channel network and morphology analysis was generated using the Topographic Analysis Kit (Forte and Whipple, 2019) and lidar topography. Channels were delineated using a minimum threshold area of $1 \times 10^3 \text{ m}^2$ to generate a stream network, which matches qualitative estimates of the smallest drainage area that convergence occurs on the hillslopes. We then calculated the slope of channel segments using the KsnChiBatch function from TAK using a channel segment length of 10 meters. Because the smallest bedrock steps, or height of outcropping lithologic units in the NW, range in size from 1-10 meters, we chose a smaller smoothing distance of 10 meters to capture finer scale changes and to match the resolution of bedrock mapping. We used the map of bedrock exposure to classify the stream

segments as a value of 1 (bedrock) and 0 (sediment mantled) based on whether the majority of a given stream segment crossed areas mapped as bedrock (Figure 6).

Using the shapefile of the stream network, we extracted slope information from the channel profiles to obtain the mean and full distribution of channel gradients in each study catchment. The slope calculations were performed for the entire channel, bare-bedrock and sediment-mantled channels by partitioning the landscape into each category based on the bedrock mapping, similar to procedures used for hillslope morphology. Using the bedrock map, I calculated the fraction of bedrock in the channels ($F_{Channel}$) by summing the length of the segments classified as bedrock (l_{Br}) and dividing by the total length of the channel (L_{Ch}) (Figure 6). I use this metric to determine how much of the channels are composed of bedrock compared to sediment mantle.

$$F_{Channel} = \frac{\sum l_{Br}}{L_{Ch}} \quad (2)$$

To compare the morphology of channels in catchments that contain the Capitan Reef to catchments without the Capitan Reef, we generated slope distribution plots of the entire channel and the channel network partitioned into bare-bedrock and sediment-mantled segments. The slope distributions for the channels in each catchment were calculated by using a kernel density smoothing function with a window size of 0.1 degrees (Figure 11).

2.4 Grain Size Analysis

Sediment grain size was determined by performing point counts from Structure-from-Motion photogrammetry (SfM) models (Figure 7) of sediment patches created from pictures in

the field. Locations for grain size mapping were focused at the base of tributaries to capture the grain size coming out of each study watershed. Sediment patches were roughly ~5 x 5 meters in size, and photos were collected using a Nikon D5500 camera or iPhone. Agisoft Photoscan was used to create the SfM models by aligning pictures of the sediment patches to create a sparse point cloud that can be processed into a dense cloud, 3D mesh, texture, and a scaled orthomosaic image (James and Robson., 2012; Neely et al. 2019). I scaled the orthomosaic by using a 15.3 cm yellow ruler placed in the pictures. The scaled orthomosaic is imported into ArcMap to perform the point count using the grid-by-number method (Bunte and Abt, 2001). A grid was created at roughly half the size of the largest boulder to measure the intermediate axis diameter of grains at the intersection points to obtain around 100 measurements for each site.

Chapter 3: Results

3.1 Bedrock mapping

Moving from WNW-ESE along the lithologic gradient in McKittrick canyon, the fraction of bedrock increases on hillslopes and in the channels (Figure 8). The hillslopes of catchments absent of the Capitan reef (1-5) have a bedrock abundance of 21%-50%, while the catchments with the reef have a smaller, but higher range of 40-53% (Figure 8). A similar trend is seen in the bedrock exposure of the channels. The channels in catchments that are not underlain by the Capitan Reef have a wide range in fraction of bedrock channels from 21%-71% compared to a smaller range of 51-71% for catchments containing the Capitan Reef unit.

3.2 Hillslope morphology

The mean hillslope angle for catchments absent of the reef have an average mean hillslope angle of $\sim 32^\circ$ while the mean hillslope angle for catchments containing the reef bedrock average $\sim 39^\circ$ (Table 1). The mean hillslope angle increases with the fraction of bedrock, with the steepest catchments (catchments 4-8) in a small range from $37-40^\circ$ with 40-53% percent of the catchment composed of bedrock. Catchments with less bedrock exposed (catchments 1-3) have a lower mean hillslope gradient $\sim 30^\circ$ with less bedrock exposed. The mean distribution of soil-mantled hillslope angle for all the catchments does not exceed 35° while the mean bedrock hillslope angle is significantly higher at 48° . The catchments underlain by the reef are steeper, with an average of 33° for sediment mantled hillslope angle while the mean bedrock hillslope angle is 45° .

3.3 Channel morphology

The fraction of bedrock in the channels increases consistently from WNW-ESE following the lithologic gradient which is consistent with the trends on the hillslopes (Figure 8). The sediment mantled channel slope without the reef averages 24° while the mean slope of bedrock channels is higher at 32° (Table 1). The increase in mean slope of the channels corresponds to an increasing abundance of bedrock as well (Figure 10B). The catchments with the reef have higher mean channel slope with an average of 30° for the sediment mantled channel slope while the mean bedrock channel slope is 35° (Figure 11). The catchments absent of the reef have a greater abundance of sediment mantled channels than bedrock channels while catchments with the reef shift to a greater abundance of bedrock channels and fewer sediment mantled channels (Figure 11). The mean slope of the channels in catchments underlain by the reef are about $\sim 5^\circ$ steeper for each partitioned segment compared to the channels in catchments absent of the reef (Figure 11).

3.4 Grain size of tributaries

The median grain size of the tributary channels increases along the WNW-ESE gradient in lithology with the smallest grain sizes found in the NW and largest grain sizes in the SE (Figure 9). There is an average median grain size of $D_{50} = 17$ cm for the catchments without the reef and an average $D_{50} = 34$ cm for the catchments that contain the reef. The increase in grain size corresponds to an increase in slope with the largest mean grain size of 54 cm found in catchment 6, which also has the steepest mean hillslope angle of 40° (Table 1). The smallest median grain sizes of $D_{50} = 8$ -15 cm are found in the catchments that do not contain the reef and have lower slopes around 30° .

Chapter 4: Discussion

4.1 Sensitivity of headwater channel slope to grain size and bedrock abundance

Both the grain size and the fraction of bedrock influence the slope of the channels in McKittrick Canyon, as seen in the positive trend of the two parameters with mean channel slope (Figure 10). Grain size and bedrock abundance play a role in setting the slope of headwater channels, but the mean slope of channels appears more sensitive to the fraction of bedrock in the channel. This can be seen in Figure 10B, where the total channel slope is most sensitive to the fraction of bare bedrock. I interpret this as indicating that the steepening of channels is accommodated primarily by increasing bare bedrock exposure rather than steepening of the bedrock or sediment-mantled channel segments.

Isolating the influence of the two parameters is complex because grain size is coupled to hillslope morphology. The grain size entering the channels is dependent on various factors of the hillslope morphology. Typically, the upstream supply of sediment influences the grain size as well, but headwater channels are in the uppermost part of the river network and in close proximity to sediment supply from hillslopes, so the grain size of headwater channels is mainly dependent on the hillslope supply. The initial size distribution of sediment is set by the fracture spacing of exhumed bedrock supplying material to the hillslope and the residence time that sediment weathers on the hillslope affects the size of sediment supplied to the channel, which connects channel morphodynamics to hillslope processes (Sklar and Dietrich, 2017).

The abundance of bedrock on the hillslopes also plays an important part in headwater channel slope because in threshold landscapes, increasing abundance of bedrock increases drives up mean catchment slope when hillslopes become insensitive to erosion rate (Neely et al, 2019),

which is also tightly correlated to colluvial channel slope (DiBiase et al., 2012). A 1:1 ratio of mean catchment slope vs channel slope for data in McKittrick Canyon and Southern California mountains shows that in both landscapes, channel slope is sensitive to the catchment slope (Figure 12). An important note is that DiBiase et al., 2012 study used mean colluvial slope, calculated by subtracting the total drainage density minus the fluvial drainage density which is classified as channels that follow the fluvial slope-area scaling (DiBiase et al., 2012). The McKittrick Canyon data does not distinguish between fluvial and colluvial drainage density. Because the catchments are typically at smaller drainage areas ($< 1 \text{ km}^2$) and at steep slopes greater than 35° , a majority of the channel network is most likely composed of headwater channels. Regardless, with increasing mean catchment slope, the slope of the channels increases at the same rate, which means that channel slope is sensitive to similar drivers of hillslope morphology.

4.2 Rock strength control on bedrock exposure

The characteristics of bedrock that composes steep, rocky cliffs is an important driver of mean catchment slope for threshold landscapes, which becomes increasingly sensitive to the strength of underlying bedrock and less sensitive to changes in erosion rate (Neely et al., 2019). In the Eastern San Gabriel Mountains (ESGM) and Northern San Jacinto Mountains (NSJM) of Southern California, the increase in mean catchment slope in NSJM is a result of more abundant, steeper cliffs from wider fracture spacing that decreases soil production efficiency and strengthens the cliffs, supporting higher relief (Neely et al., 2019). The strength of the underlying bedrock, set by the fracture spacing and competency of exhumed rock, affects when bedrock is

exposed, and thus the slope of the catchments. McKittrick Canyon plots in a similar trend as data from Southern California (Figure 13), but plots slightly above the data suggesting more bedrock exposed for a given slope. The difference could be a result of the landscapes differing lithology. The Southern California mountains are underlain by granitic rocks while McKittrick Canyon is underlain by layered sedimentary rocks. Because McKittrick Canyon has more bedrock exposure, this could mean a lower soil production efficiency in this landscape.

In McKittrick Canyon, qualitatively observing the morphology of cliffs in the NW compared to the SE, the smaller cliffs in the NW appear more fractured than the massive cliffs in the SE. The change in lithology from interbedded carbonates and siliciclastic to predominantly massive carbonate reef units from NW-SE corresponds to a greater abundance of bedrock in catchments and in the channels, seen by the increase in bedrock exposure with the presence of the reef (Figure 8). While the variation in fracture density between ESGM and NSJM is most likely due to differences in tectonic activity (DiBiase et al., 2018), McKittrick Canyon has no knickpoints or features to suggest changes in tectonic activity along the canyon, so the change in fracture spacing of cliffs in this landscape must have a different explanation, most likely due to differences in lithology or bed thickness.

4.3 Lithologic control on bedrock exposure and fracture spacing in McKittrick Canyon

In McKittrick Canyon, the change in fracture spacing and bedrock exposure along the NW-SE gradient is most likely driven by changes in bed thickness resulting from a transition in lithology. In the NW end of the canyon, the dominant lithology is the Carlsbad limestone unit, a thin bedded limestone with sandstone members which transitions to the Capitan limestone unit, a

thick to massively bedded limestone unit (Figure 5). The massive carbonate units maybe harder to weather and more competent, seen in the decreased fracturing of the cliffs and decrease increase in bedrock exposure. Many of the catchments are at threshold similar to the catchments in southern California, which means that catchment slope increases in response to increased bedrock exposure rather than erosion rates. In McKittrick Canyon, the massive carbonate cliffs are steep and take up a greater amount of the catchment, this can explain the increase in catchment slope moving WNW-ESE in the canyon.

Differential erosion between the sandstone/siliciclastic and carbonate rock layers could be a mechanism that influences soil production as well. Based on fieldwork, a majority of the outcropping bedrock are the thin bedded carbonates in the NW and the massive reef units in the SE, suggesting that the siliciclastic could be more efficient at weathering in this climate. While we assume that erosion rates are equal along the canyon because of the small spatial extent and no knickpoints to suggest that the landscape is responding at different rates to perturbations, spatial variation in the erodibility of lithologic units can cause changes in landscape form that create variability in erosion rates (Forte et al., 2016). In the case of McKittrick Canyon, catchments 1, 2 and 3 are not yet at threshold slopes and primarily underlain by the Carlsbad limestone, a weaker unit than the Capitan Limestone. Future work could include careful mapping of the siliciclastic units and carbonate units to determine if the onset of bedrock exposure is mainly due to the presence of carbonate units and if there are differences in erosion rate between the Carlsbad and Capitan limestone units.

Chapter 5: Conclusion

The lithologic gradient in the Guadalupe mountains plays an important part in changing the strength of underlying bedrock that influences the grain size and bedrock exposure in the catchments and the channels. Headwater channel morphology is tightly coupled to the dynamics of hillslope morphology, with the effect of grain size from nearby cliffs influencing the slope of the sediment-mantled parts of the channel, while the amount of bedrock exposure changes in response to decreased fracture spacing of the adjacent carbonate cliffs reduces soil production efficiency. The gradient of the headwater channels in this landscape appears more sensitive to the amount of the channel composed of bedrock, which increases in catchments moving NW-SE McKittrick Canyon as a result of a greater abundance of carbonate units. The stratal architecture of the lithologic units sets the relief and fracture spacing of the cliffs with thicker beds in the Capitan limestone having a greater competency and strength than the thinner carbonate beds in the Carlsbad limestone in the NW catchments. This study suggests that headwater channels in threshold landscapes become increasingly sensitive to variability in the underlying rock strength of the hillslopes.

BIBLIOGRAPHY

- Ahnert, F., 1970. Functional relationships between denudation, relief, and uplift in large, mid-latitude drainage basins. *American Journal of Science*, 268(3), pp.243-263.
- Attal, M., Mudd, S.M., Hurst, M.D., Weinman, B., Yoo, K. and Naylor, M., 2015. Impact of change in erosion rate and landscape steepness on hillslope and fluvial sediments grain size in the Feather River basin (Sierra Nevada, California). *Earth Surface Dynamics*, 3(1), pp.201-222.
- Benda, L., Hassan, M.A., Church, M. and May, C.L., 2005. Geomorphology of steep-land headwaters: the transition from hillslopes to channels 1. *JAWRA Journal of the American Water Resources Association*, 41(4), pp.835-851.
- Benda, L. and Dunne, T., 1997. Stochastic forcing of sediment supply to channel networks from landsliding and debris flow. *Water Resources Research*, 33(12), pp.2849-2863.
- Bunte, K. and Abt, S.R., 2001. Sampling Frame For Improving Pebble Count Accuracy In Coarse Gravel-Bed Streams. *JAWRA Journal of the American Water Resources Association*, 37(4), pp.1001-1014.
- Clarke, B.A. and Burbank, D.W., 2011. Quantifying bedrock-fracture patterns within the shallow subsurface: Implications for rock mass strength, bedrock landslides, and erodibility. *Journal of Geophysical Research: Earth Surface*, 116(F4).
- DiBiase, R.A., Heimsath, A.M., Whipple, K.X., 2012. Hillslope response to tectonic forcing in threshold landscapes. *Earth Surf. Process. Landf.* 37 (8), 855–865. <https://doi.org/10.1002/esp.3205>.

- DiBiase, R.A., Rossi, M.W. and Neely, A.B., 2018. Fracture density and grain size controls on the relief structure of bedrock landscapes. *Geology*, 46(5), pp.399-402.
- Forte, A.M., Yanites, B.J. and Whipple, K.X., 2016. Complexities of landscape evolution during incision through layered stratigraphy with contrasts in rock strength. *Earth Surface Processes and Landforms*, 41(12), pp.1736-1757.
- Forte, A.M. and Whipple, K.X., 2019. The topographic analysis kit (TAK) for TopoToolbox. *Earth Surface Dynamics*, 7(1), p.87.
- Hack, J.T., 1960. Interpretation of erosional topography in humid temperate regions. *Bobbs-Merrill*.
- Hill, C.A., 2000. Overview of the geologic history of cave development in the Guadalupe Mountains, New Mexico. *Journal of Cave and Karst Studies*, 62(2), pp.60-71.
- Howard, A.D., 1994. A detachment-limited model of drainage basin evolution. *Water resources research*, 30(7), pp.2261-2285.
- Hsu, L., Dietrich, W.E. and Sklar, L.S., 2008. Experimental study of bedrock erosion by granular flows. *Journal of Geophysical Research: Earth Surface*, 113(F2).
- King, P.B., 1942. Permian of West Texas and Southeastern New Mexico: PART. *AAPG Bulletin*, 26(4), pp.535-649.
- Kirby, E. and Whipple, K.X., 2012. Expression of active tectonics in erosional landscapes. *Journal of Structural Geology*, 44, pp.54-75.
- Lague, D. and Davy, P., 2003. Constraints on the long-term colluvial erosion law by analyzing slope-area relationships at various tectonic uplift rates in the Siwaliks Hills (Nepal). *Journal of Geophysical Research: Solid Earth*, 108(B2).
- Leopold, L.B., 1970. An improved method for size distribution of stream bed gravel. *Water*

- Resources Research, 6(5), pp.1357-1366.
- James, M. R., and Robson, S., 2012. Straightforward reconstruction of 3D surfaces and topography with a camera: Accuracy and geoscience application. *J. Geophys. Res.*, 117, F03017, doi:10.1029/2011JF002289.
- Neely, A.B., DiBiase, R.A., Corbett, L.B., Bierman, P.R. and Caffee, M.W., 2019. Bedrock fracture density controls on hillslope erodibility in steep, rocky landscapes with patchy soil cover, southern California, USA. *Earth and Planetary Science Letters*, 522, pp.186-197.
- Neely, A. (2019). Quantifying rock strength controls in Guadalupe Mountains, NM/TX. National Center for Airborne Laser Mapping (NCALM). Distributed by OpenTopography. <https://doi.org/10.5069/G9BK19G8>. Accessed: 2020-04-29
- Penserini, B.D., Roering, J.J. and Streig, A., 2017. A morphologic proxy for debris flow erosion with application to the earthquake deformation cycle, Cascadia Subduction Zone, USA. *Geomorphology*, 282, pp.150-161.
- Prancevic, J.P., Lamb, M.P. and Fuller, B.M., 2014. Incipient sediment motion across the river to debris-flow transition. *Geology*, 42(3), pp.191-194.
- Schmidt, K.M. and Montgomery, D.R., 1995. Limits to relief. *Science*, 270(5236), pp.617-620.
- Shobe, C.M., Tucker, G.E. and Anderson, R.S., 2016. Hillslope-derived blocks retard river incision. *Geophysical Research Letters*, 43(10), pp.5070-5078.
- Sklar, L.S. and Dietrich, W.E., 2001. Sediment and rock strength controls on river incision into bedrock. *Geology*, 29(12), pp.1087-1090.
- Sklar, L.S. and Dietrich, W.E., 2004. A mechanistic model for river incision into bedrock by saltating bed load. *Water Resources Research*, 40(6).

- Sklar, L.S., Riebe, C.S., Marshall, J.A., Genetti, J., Leclere, S., Lukens, C.L. and Mercres, V., 2017. The problem of predicting the size distribution of sediment supplied by hillslopes to rivers. *Geomorphology*, 277, pp.31-49.
- Smith, B.P. and Kerans, C., 2018. Interpreting stratal architecture in shelf-top carbonate systems: an example from the seven rivers formation, McKittrick Canyon, New Mexico, USA. *Journal of Sedimentary Research*, 88(4), pp.475-494.
- Stock, J. and Dietrich, W.E., 2003. Valley incision by debris flows: Evidence of a topographic signature. *Water Resources Research*, 39(4).
- Stock, J.D. and Dietrich, W.E., 2006. Erosion of steepland valleys by debris flows. *Geological Society of America Bulletin*, 118(9-10), pp.1125-1148.
- Tinker, S.W., 1998. Shelf-to-basin facies distributions and sequence stratigraphy of a steep-rimmed carbonate margin: Capitan depositional system, McKittrick Canyon, New Mexico and Texas. *Journal of Sedimentary Research*, 68(6).
- Whipple, K.X. and Tucker, G.E., 1999. Dynamics of the stream-power river incision model: Implications for height limits of mountain ranges, landscape response timescales, and research needs. *Journal of Geophysical Research: Solid Earth*, 104(B8), pp.17661-17674.
- Yohannes, B., Hsu, L., Dietrich, W.E. and Hill, K.M., 2012. Boundary stresses due to impacts from dry granular flows. *Journal of Geophysical Research: Earth Surface*, 117(F2).

Table 1: Median grain size, partitioned hillslope morphology, and partitioned channel morphology.

ID (Fig. 1)	Drainage area (km ²)	Mean Hillslope Angle (°)	Mean Channel Slope (°)	Mean Bedrock Hillslope Angle (°)	Mean Bedrock Channel Slope (°)	Mean Soil- Mantled Hillslope Angle (°)	Mean Sediment- Mantled Channel Slope (°)	Fraction Channel Bedrock, F_{channel}	Fraction Bedrock Hillslopes, $F_{\text{catchment}}$	D ₅₀ (cm)	Distance Downstream of catchment 1 (km)
A	2.2	25.7	21.65	35.25	27.06	23.38	19.53	0.28	0.21	8.5	0
B	2.1	30.7	27.85	35.89	30.93	28.03	25.81	0.40	0.28	15.8	0.55
C	0.62	29.8	28.29	42.79	34.13	24.87	22.78	0.49	0.29	28.1	1.5
D	0.1	37.2	29.83	42.14	32.48	32.67	25.08	0.64	0.50	-	2.00
E	0.47	37	32.83	41.45	34.66	34.24	28.44	0.71	0.40	15.6	2.9
F	0.35	40.6	33.64	48.88	35.06	35.13	31.72	0.57	0.40	57.5	5.9
G	0.21	38.9	34.20	45.55	36.57	31.82	28.50	0.71	0.52	29	6.3
H	0.43	37.8	33.06	41.92	33.83	33.31	30.42	0.77	0.53	32.4	9.8

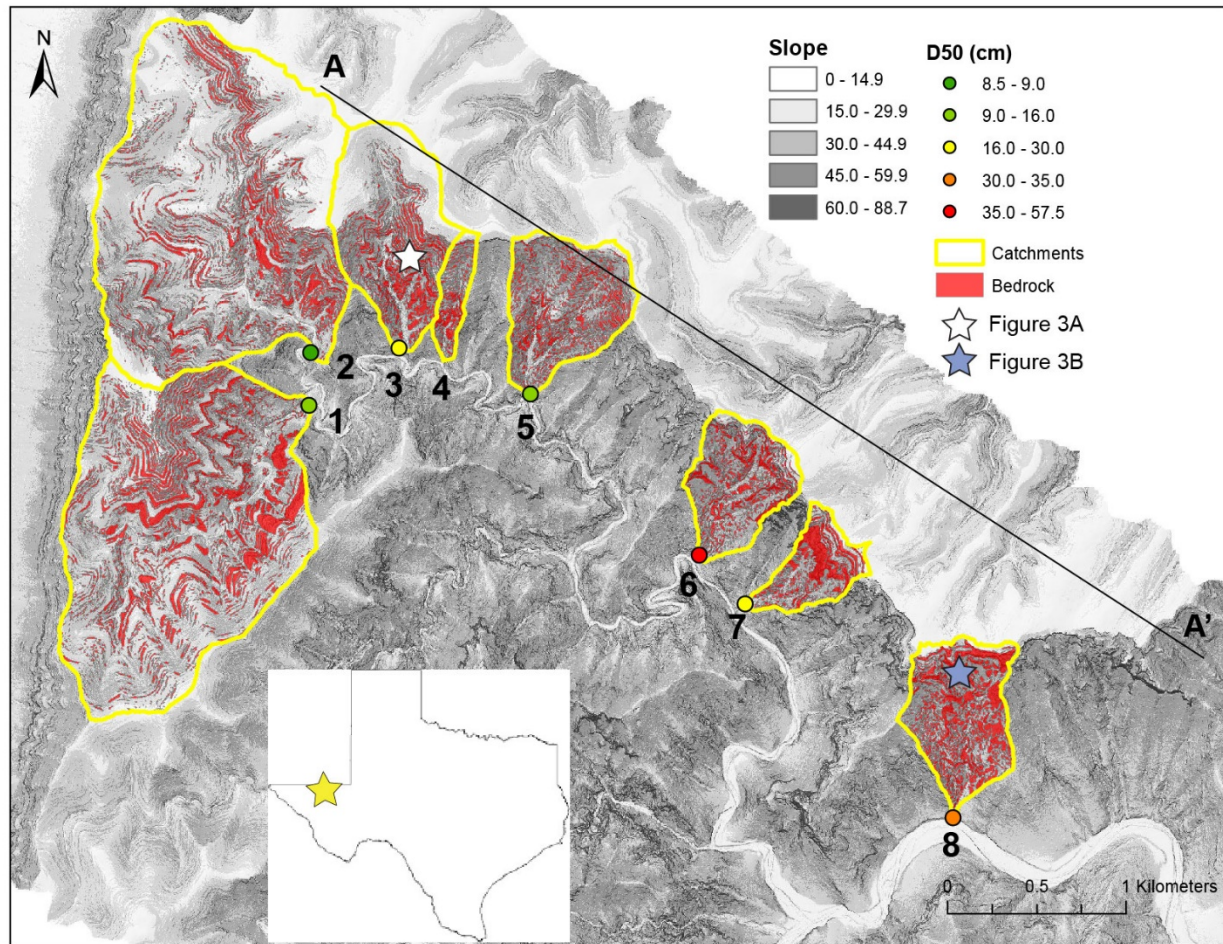


Figure 1: Grain size analysis conducted for 7 of the catchments (excluding 4) with the median grain size (D_{50}) calculated for for each survey. Detailed bedrock mapping of the hillslopes and channels of the 8 catchments outlined in red polygons at a ~ 50 cm scale resolution. The star symbols represent location of photographs in Figure 3A and Figure 3B.

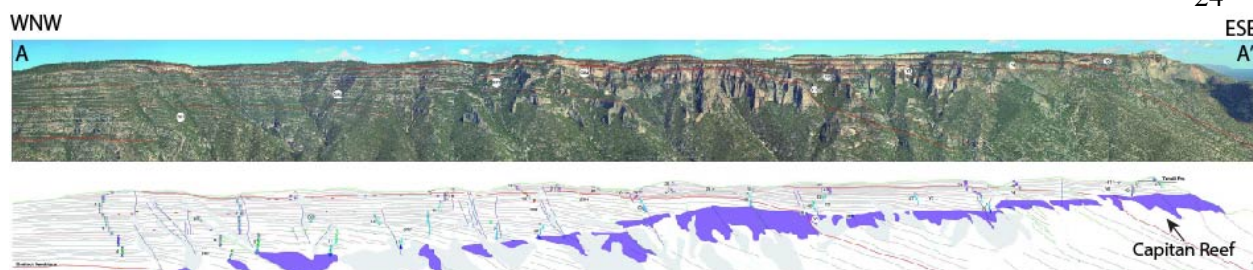
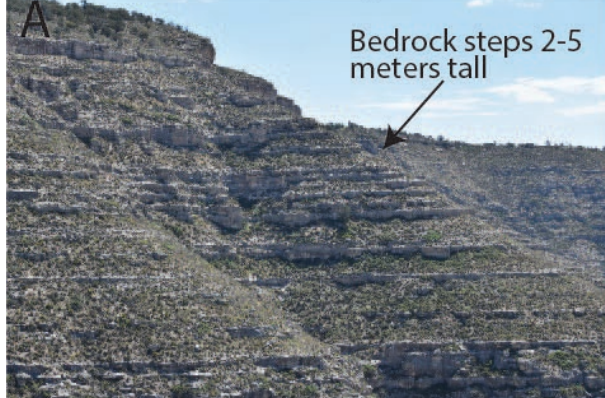


Figure 2: Panorama of McKittrick Canyon (modified from Tinker et al., 1998) with the extent outlined in the overview map (Figure 1) by the cross section of A-A'. Top panel shows the transition from small, even beds in the WNW to more massive reef units in the ESE. Bottom panel outlines the prograding Capitan Reef (purple) that shifts higher into the catchments with distance to the ESE.

Hillslope on NW end of Canyon



Hillslope on SE end of Canyon



Figure 3: Location of pictures located at the star symbols on Figure 1. The NW end of McKittrick Canyon has laterally continuous, 2-5 meter tall bedrock cliffs (A) that transition into massive reef units up to 100 meters tall in the SE end of the canyon (B).

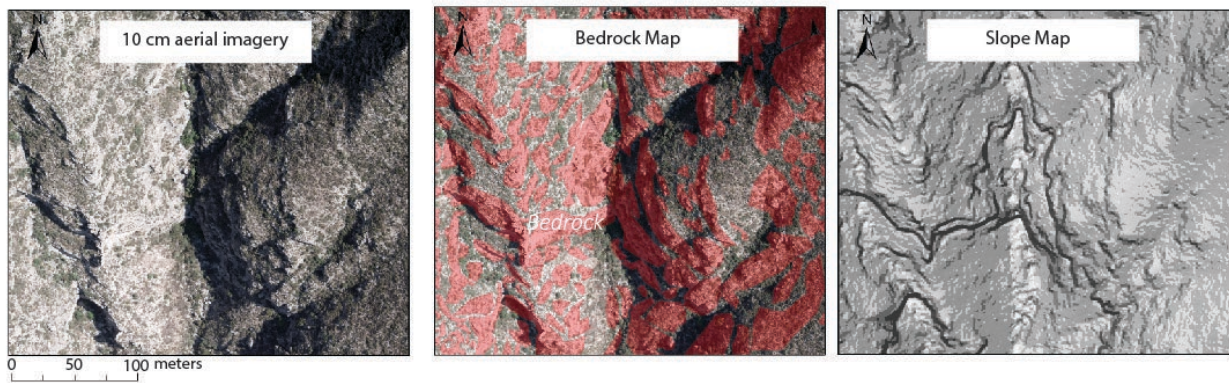


Figure 4: Bedrock mapping consisted of using the aerial imagery (far left panel) to identify areas of exposed bedrock and outline in a polygon to calculate the slope of the partitioned catchment using the slope map (far right panel)

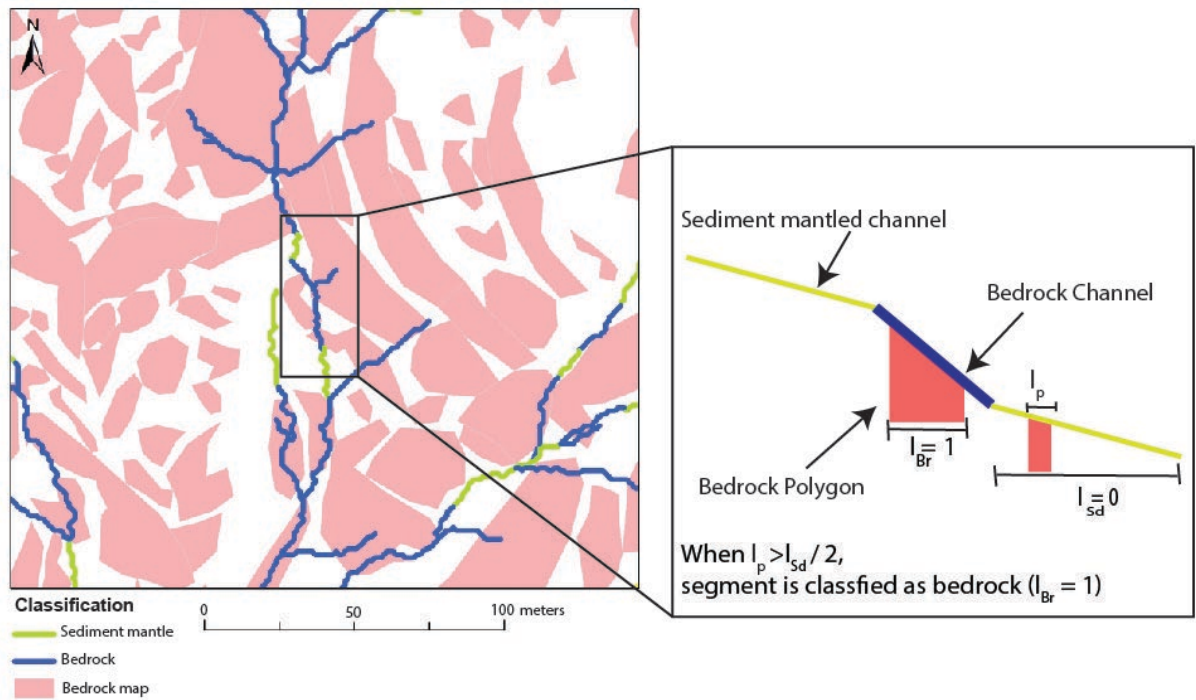


Figure 5: Partitioning of the channels based on the intersection of the channel segments with bedrock map. To classify as a bedrock channel, a majority of the channel segment must overly mapped bedrock.

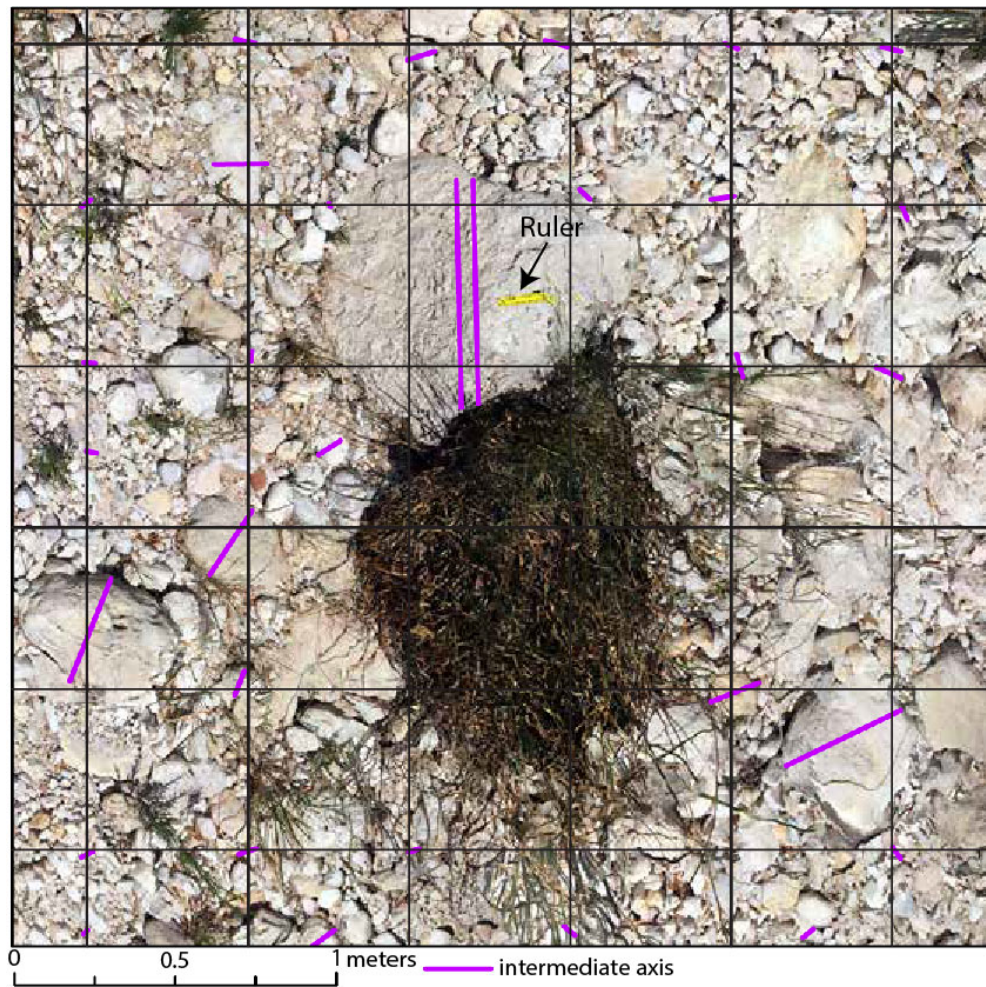


Figure 6: Structure-from-Motion derived orthomosaic image of sediment patch with a 0.5 m grid spacing overlain. Purple lines indicate measurements of apparent intermediate axis diameter.

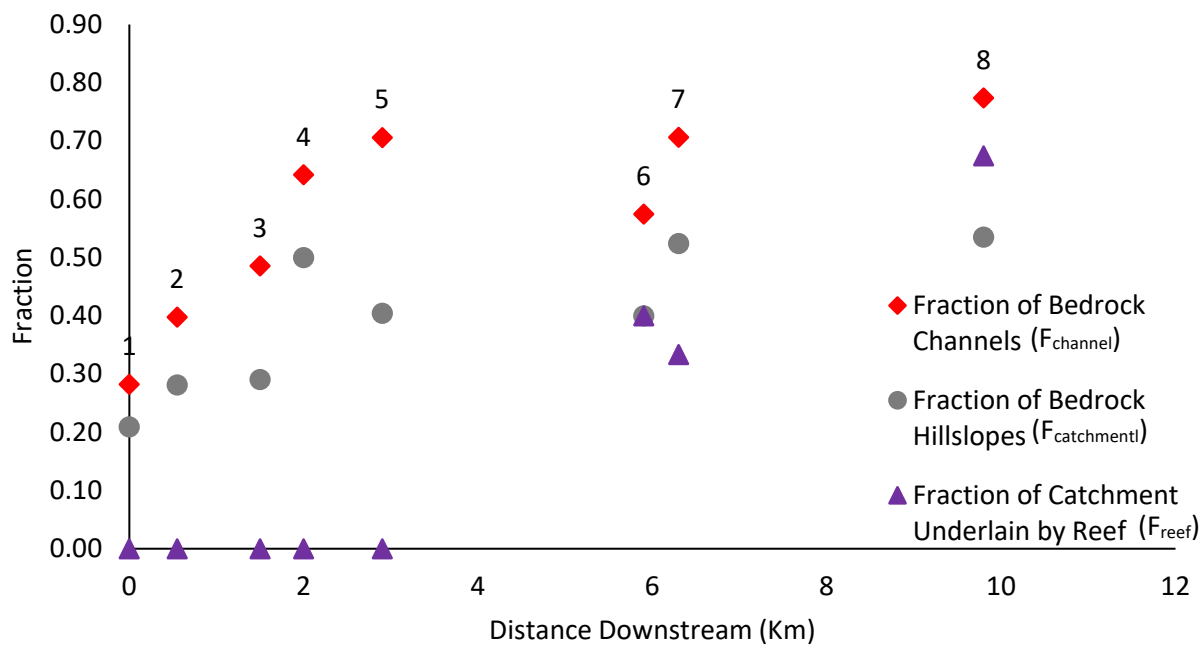


Figure 7: Fraction of bedrock vs distance downstream from catchment 1 along WNW-ESE lithologic gradient. The fraction of the catchment underlain by the Capitan reef is included on the plot to show how the abundance of bedrock changes with the presence of the reef.

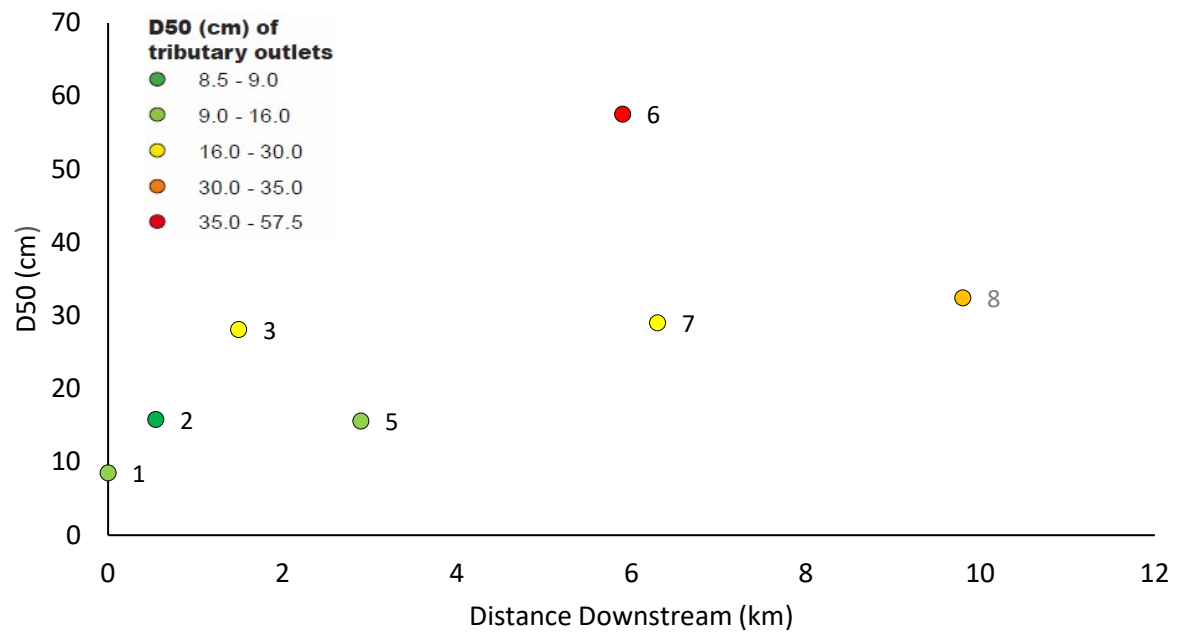


Figure 8: Median grain size, D_{50} , versus Distance Downstream of Catchment 1 along WNW-ESE gradient in lithology. No grain size data available for Catchment 4.

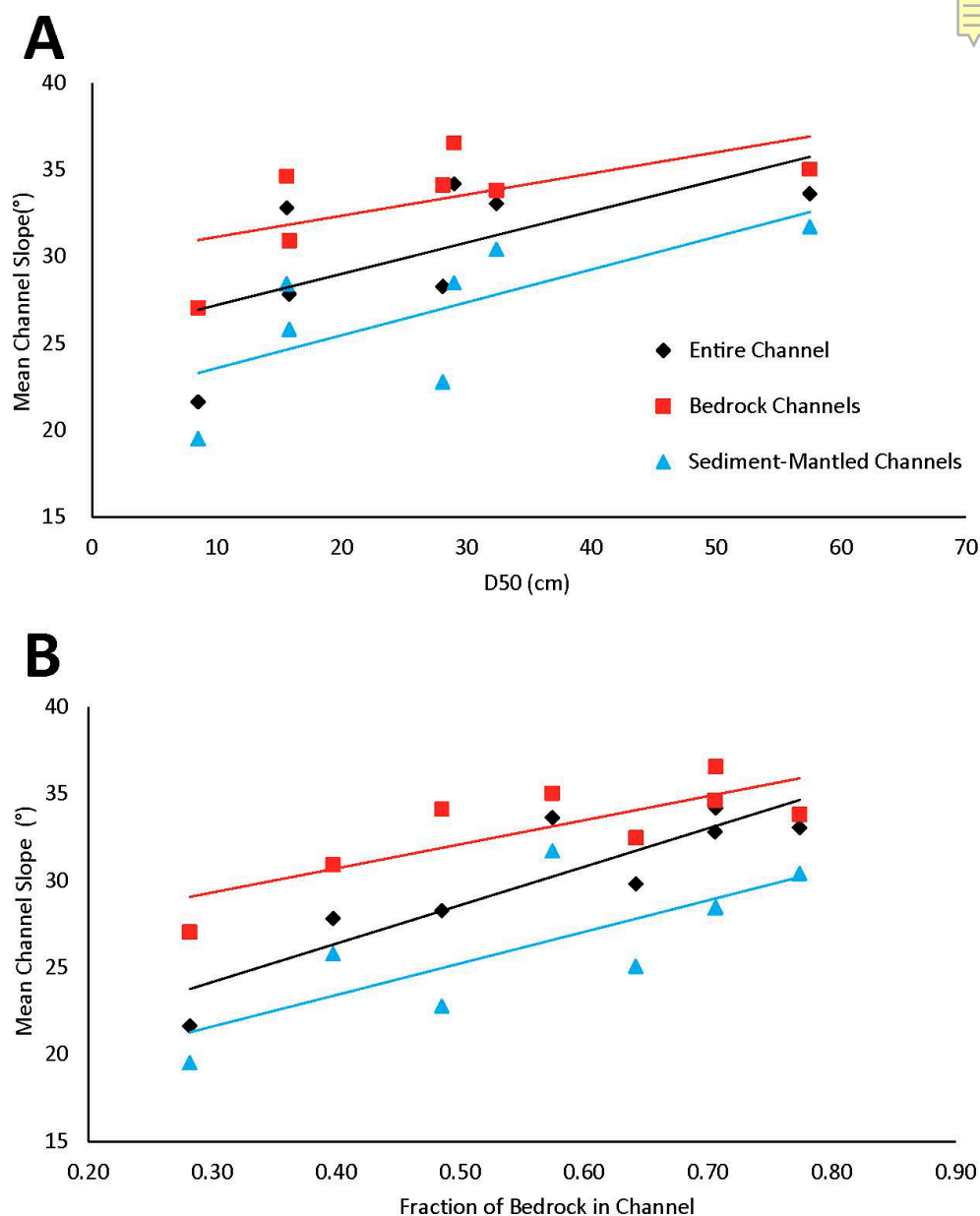


Figure 9: (A) Mean Channel Slope versus Median grain size, D_{50} , for the partitioned channels to see how slope changes compared to the grain size in each catchment. (B) Mean Channel Slope versus Fraction of bedrock for the partitioned channels to see how the slope changes for with bedrock exposure.

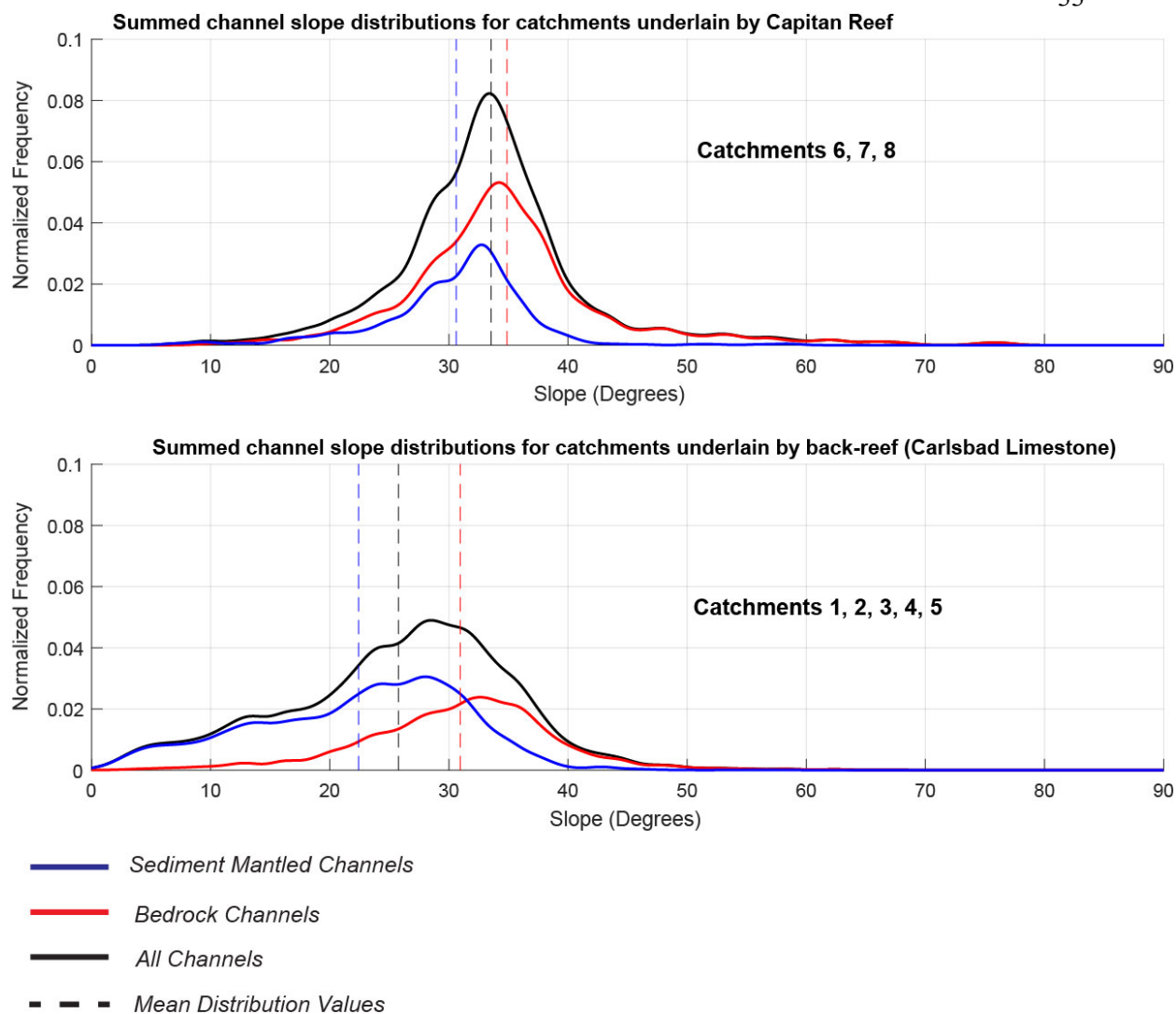


Figure 10: Kernel density plots of channel slope angle separated by whether the catchments contain the Capitan reef (Top panel) or do not contain the reef (bottom panel). The dashed line represents the mean angle of the partitioned channel slopes. Area under the curve represents the abundance of slopes classified as either bedrock or sediment-mantled.

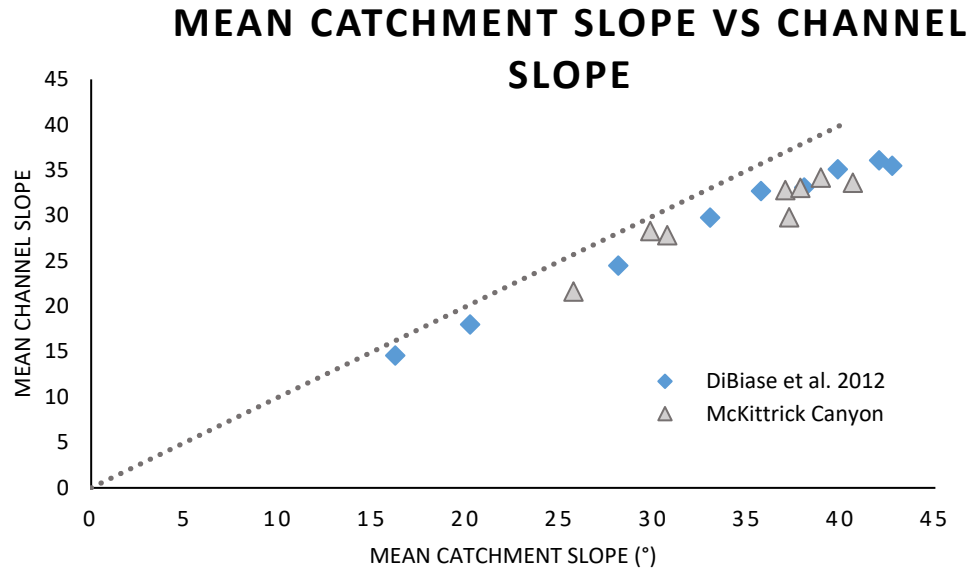


Figure 11: Mean catchment slope versus mean channel slope for McKittrick Canyon data compared against data in Southern California (DiBiase et al., 2012). Dashed line represents a 1:1 relationship. The channel slope for DiBiase et al., 2012 is calculated by using a linear fit to each colluvial channel in the catchments, and averaging all such channels for each catchment, weighted by mean channel length. McKittrick Canyon data averages over all channel segments in a given catchment, weighted by mean channel length.

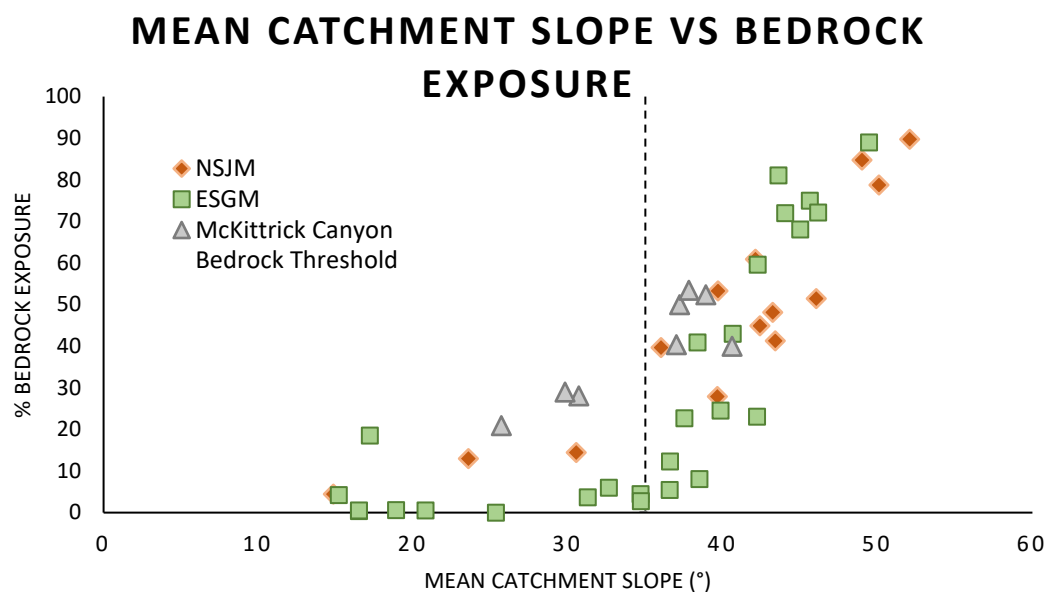


Figure 12: Mean Catchment slope vs percent bedrock exposure for McKittrick Canyon data (Table 1) compared to data from Southern California in the Eastern San Gabriel Mountains (ESGM) and Northern San Jacinto Mountains (NSJM) (Neely et al., 2019).

EDUCATION

May 2020

B.S in Geoscience with Minor in Mathematics
Pennsylvania State University, Schreyer Honor College

TEACHING AND RESEARCH EXPERIENCE

2019—Present

Senior Thesis Research

Title: The Influence of changing lithology on the bedrock hillslope morphology along a WNW-ESE trending exposure in McKittrick Canyon
Quantified rock type controls on the morphology of bedrock hillslopes and debris flow channel morphology in McKittrick Canyon, Guadalupe Mountains, NM/TX, using lidar topography, structure-from-motion photogrammetry, and field surveys

2019—Present

East African Rift Tephra Database (EarthD) Collaborator

Compile data from papers documenting geochemistry of tephra samples from the East African Rift Valley into a comprehensive database as part of the NSF-funded Earth-D project (EAR-1753738)

2019

Teaching Intern, Department of Geoscience

Helped students with ArcGIS exercises during weekly lab sessions for Geosci 340 (Geomorphology class)

2018—2019

Part-time Research Support

Built 3D models of bedrock hillslopes using structure-from-motion photogrammetry to quantify heterogeneity in bedrock hillslopes at the landscape scale, as part of an NSF funded project (EAR-1608014) focused on quantifying fracture controls on bedrock hillslope morphology in Southern California

2017—2018

Women in Science and Engineering Research Intern

Analyzed petrographic thin sections of basalts from the East African Rift by identifying minerals and characteristics of the rocks
Studied the geochemistry of Miocene basalts from Saudi Arabia using electron microprobe analysis to determine the origin of basalt magmatism

FIELD EXPERIENCE

2019

GSA/ExxonMobil Bighorn Basin Field Award

	Field Seminar in the Bighorn Basin, WY emphasizing multi-disciplinary basin analysis
2019	Penn State Field Camp Six-week capstone field course for geoscience majors in Montana, Wyoming, Idaho and Utah
2019	Field Work for Senior thesis Surveyed hillslopes and channels in McKittrick Canyon, Guadalupe Mountains, collecting grain size data and imagery to generate 3D models from structure-from-motion photogrammetry
2018	Field Assistant in Taiwan Central Range Assisted Penn State PhD student Julia Carr in conducting drone surveys and mapping of river corridors in the Taiwan Central Range

CONFERENCE ABSTRACTS

Loucks, E., Neely, A.B., and DiBiase, R.A., 2019. The influence of rock properties on the morphology of headwater channels in the Guadalupe Mountains, TX. Abstract EP53E- 2219, presenting at 2019 Fall Meeting, AGU, San Francisco, CA, 9-13 Dec.

Loucks, E., Neely, A.B., and DiBiase, R.A., 2018. Using ground-based structure-from-motion photogrammetry to quantify heterogeneity in bedrock hillslope morphology. Abstract EP53E- 1930, presented at 2018 Fall Meeting, AGU, Washington, DC, 10-14 Dec.

HONORS AND AWARDS

	<u>From the Department of Geoscience</u>
2019	Timothy and Courtney Watson Undergraduate Scholarship
2019	Demshur UG Research Geoscience
2019	Vaugh Field Trip Fund
2018	John and Elizabeth Holmes Teas Scholarship Fund
2018	Ronald A. Landon Endowment in Hydrogeology
	<u>From Schreyer Honors College</u>
2018	Gerald Bayles Memorial Scholarship
2017	Van Dyke Memorial Scholarship
2017	John C. and Nancy Griffiths Scholarship
2017	Robert F. Schmalz Award
2016	Academic Excellence Scholarship
	<u>From the College of Earth and Mineral Sciences</u>
2016-2017	Mathew J Wilson Honors Scholarship
	<u>From Penn State</u>
2016-2019	University Park Provost Scholarship
	<u>Outside Scholarships</u>
2016-2020	Bissel Smith Scholarship
2016-2020	Philip E. Potter Foundation Scholarship